Open Journal of Science & Technology
Journal Homepage: http://readersinsight.net/OJST

Research Article

Energy dissipation capacity of precast concrete beam-column joint connected by double notch subjected to cyclic lateral loading

Ruminsar Simbolon[1]*, Herman Parung[2], Rita Irmawaty[3], dan Arwin Amiruddin[4]

[1]Civil Engineering, Hasanudin Universitas, Kemerdekaan, Indonesia.
[2,3,4]Departement Teknik Sipil, Hasanudin Universitas, Kemerdekaan, Indonesia.

*Corresponding Author email: ruminsar_15@yahoo.co.id

Submission: 13 October 2020 *Revised: 04 July 2021* *Accepted: 22 July 2021*

ABSTRACT

This paper presents the experimental investigation of full-scale precast concrete beam-column connections subjected to cyclic lateral loading. The specimen consists of three models. Two of which are precast beam-column connections and one is monolith. The precast and monolith specimen were designed for the same strength. The cross-sectional dimensions of the beam 250 mm x 300 mm and column 300 mm x 300 mm. Connections are placed in plastic hinge area, with a distance of h (beam height) from the face of the column which is expected to occur first destruction. Precast construction joints are distinguished, with 3 different models, namely monolith, double notch type 1 (STR-1), and double notch type 2 (STR-2). Maximum load capacity, hysterical behavior and energy dissipation are measured, and capacity is compared. The results showed that beam-column joint STR-2 are better able to absorb energy than beam column joint monolith and beam-column joint STR-1. Kumulative energy dissipation of monolith about 9333.07 kN-mm, STR-1 is 8336.76 kN-mm, and STR-2 is 10162.52 kN-mm. The use of dual notch connections (STR-1 and STR-2) provides satisfactory performance, which is marked by meeting the minimum relative energy dissipation ratio at a 3.5% drift according to the ACI Committee 374.1-05. The results show that the STR-2 beam-column connection is more capable of absorbing energy than the monolith beam-column connection and STR-1 beam connection. the value of monolithic cumulative energy dissipation is around 9333.07 kN-mm, STR-1 is 8336.76 kN-mm, and STR-2 is 10162.52 kN-mm. in principle, all three test specimens, monoliths, STR-1 and STR-2 provide satisfactory stability performance under lateral cyclic loads, because they still meet the minimum relative energy dissipation ratio at a deviation of 3.5% according to the ACI Committee 374.1 -05

Keywords: *Cyclic Loading; Monolith; Precast Concrete; Beam-Column Connection; Symmetrical Double Notch; Non Simetrical Double Notch*

1. INTRODUCTION

Precast concrete cannot be widely used because the reliability of connections between elements is still an obstacle, especially against earthquake loads (1). Indonesia due to its location and geographical conditions are often hit by large earthquakes, causing the use of precast concrete construction is very risky (2). Based on public works department sources, there are several types of systems precast column beam joints developed in Indonesia (3).

https://doi.org/10.31580/ojst.v4i2.1675

This paper proposes a type of precast beam-column connection, which is symmetrical and asymmetrical double notch joints. The connection between the column and the precast beam through splicing reinforcement, which is inserted into the hole provided and then filled with non-shrinking grouting material loading which is reviewed in this experimental study is repeated (cyclic) lateral loading. Modeling boundary conditions follows the portal deformation pattern due to lateral loads, where the zero moment in the column is located in the middle of the column between the floors, and the zero moment in the beam occurs in the center of the span (4). The purpose of this study is to determine the value of energy dissipation from monolith test specimens and multiple notch test specimens in the connection of precast concrete beam-column joints, due to cyclic lateral loads.

2. LITERATURE REVIEW

2.1. ENERGY DISSIPATION CAPACITY

Energy dissipation capacity is defined as the energy absorbed (total energy received by the structure) reduced by elastic energy in each repetitive loading cycle, where the structure maintains its strength through the mechanism of damage in the form of structural cracks and melting reinforcement (5). The energy dissipation of concrete structures is one of the fundamental capacities that determines the structure's resistance to earthquake loads (5). It is found that the failure mechanism of reinforced concrete structures not only dependent on the loading path and the history of crack formation, but it is also affected by the presence of relatively low energy dissipation during the seismic event (6). If structural parts have low energy dissipation, there may be inadequate structural attenuation. In addition, oscillations can also continue for a long time after an earthquake, resulting in a fatigue effect at low cycles, and lateral displacement may be excessive (7). Therefore it is important to determine the minimum energy dissipation requirements that can be tolerated in structural members when subjected to earthquake loads. In this case the calculation of energy dissipation refers to ACI 374.1-05 (1). The amount of dissipation energy for each loading cycle is calculated as the area of the area bounded by the load deflection hysteresis loop in the third cycle structure for each drift ratio value. The definition of energy absorption and energy disposal as shown in Fig. 1.

$$E_a = E_e + E_d \ldots\ldots\ldots \quad (1)$$

Where

E_a = Absorbed Energy;

E_e = Elastic Energy

E_d = Dissipation Energy.

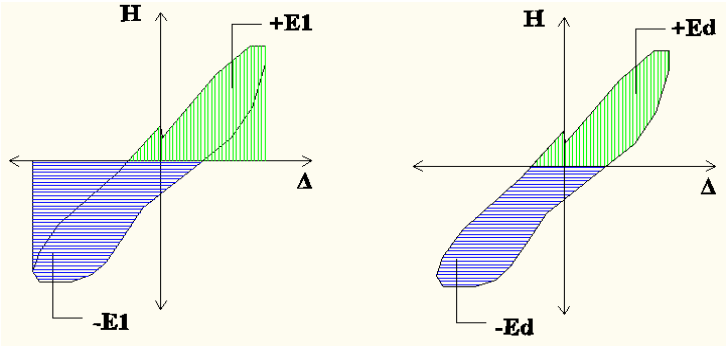

Fig. 1. Energy total and energy dissipation

2.2. Relative Energy Dissipation

The relative energy dissipation is defined as the ratio of actual to ideal energy dissipated by test speciment during reversed cyclic response between given drift ratio limits as shown in Fig. 2 (8). The actual energy dissipation is expressed as the area in the hysteretic loop per load cycle and can be calculated by referring to the Equation 2 (9).

$$E_n = \sum_{i=1}^{n} \left(\frac{F_i + F_{i+1}}{2}\right) x \Delta_x \qquad (2)$$

where:

E_n = *actual* energy dissipation in *n* increment of drift ratio

Δ_x = deviation of two displacements, *xi*+1 - *xi*

F_i = lateral load at the beginning of incremental displacement

F_{i+1} = lateral load at the end of incremental displacement

The ideal energy dissipation is defined as the area of the circumscribing parallelograms ABCD and DEFA in the elastoplastic condition during the third cycle of 3.5% drift ratio. These parallelograms are formed according to the following process:

1. the slope lines AB and CD are parallel to OA1, representing the initial stiffness in the positive direction (line AB for loading and CD for unloading);
2. the slope lines FA and DE are parallel to OA2, depicting the initial stiffness in the negative direction (line DE for reversed loading and FA for unloading);
3. lines BC and EF describe the peak lateral load in the loading and reversed loading condition respectively.

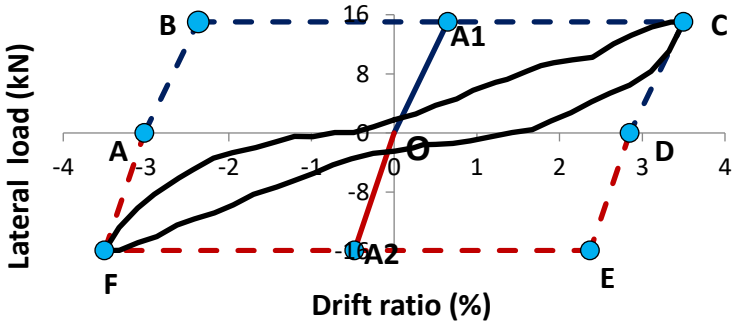

Fig. 2. Ideal energy dissipation

The ideal energy dissipation and relative energy dissipation can be calculated by referring to the Equation 3 and 4

$$E_i = (x_c - x_b)y_c + (x_e - x_f)y_f \ldots \quad (3)$$

$$E_r = \frac{E_i}{E_n} \ldots\ldots\ldots \quad (4)$$

where:

Ei = *Ideal* energy dissipation

Er = *relative* energy dissipation of drift ratio 3.5%

3. METHODOLOGY/MATERIALS

3.1. Material Properties

Deformed rebar with a yield strength of 400 MPa is used. D16 is used as the main reinforcement of the column and D13 as the main reinforcement of the beam. for stirrup reinforcement used Ø8. To measure the properties of reinforcement, three specimens were tested according to ASTM-A370. The results are shown in Table 1. Concrete is designed to have a compressive strength of 25 MPa, with a maximum aggregate size of 25 mm and a slump of 120 mm. To determine the compressive strength of concrete, ten specimens were tested on the same day as foundry, according to ASTMC39. The test results for compressive strength of concrete are summarized in Table 2.

Table 1. Properties of the rebar.

Type	Yield tensile strength (fy, MPa)	Ultimate tensile strength (fu, MPa)	Elastic modulus (MPa)
Ø8	312	487	$2{,}04 \times 10^5$
Ø10	319	492	$2{,}03 \times 10^5$
D13	430	585	$2{,}04 \times 10^5$
D16	414	574	$2{,}01 \times 10^5$

Table 2. Properties of the rebar.

Test result		
Design strength (MPa)	**Comressive strength (MPa)**	**Elastic modulus (MPa)**
25	24,3	$2{,}01 \times 10^4$

3.2. Reinforcement Details

The specimen is an exterior beam-column in a 5-storey building. The length of the beam represents half the length of the bend span. column height represents the height of the column from the height of one floor to the middle height of the next floor. Boundary conditions are set to simulate counter-bending points on beams and columns with acceptable accuracy. Fig. 3 shows the dimensions and details of the test specimen. reinforcement of all three specimens is designed and detailed according to ACI 318-08. Strength in the joints is expected to be contributed by the concrete notch system, grouting installation on the reinforcement, and channel forces by utilizing flexural and shear reinforcement.

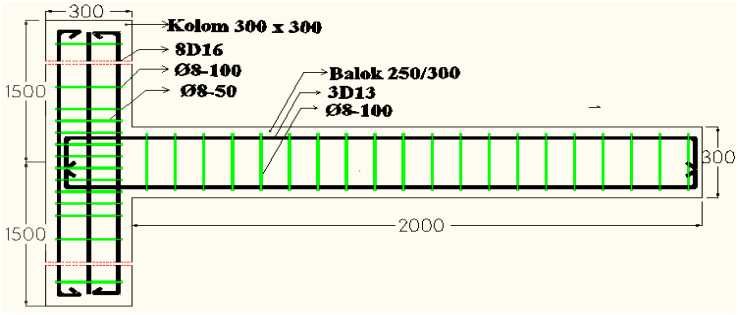

(a) monolith

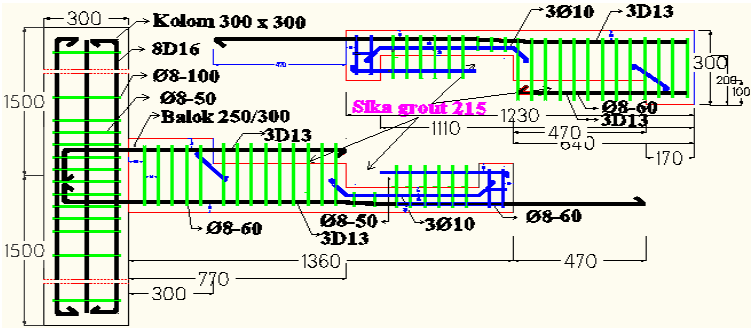

(b) STR-1

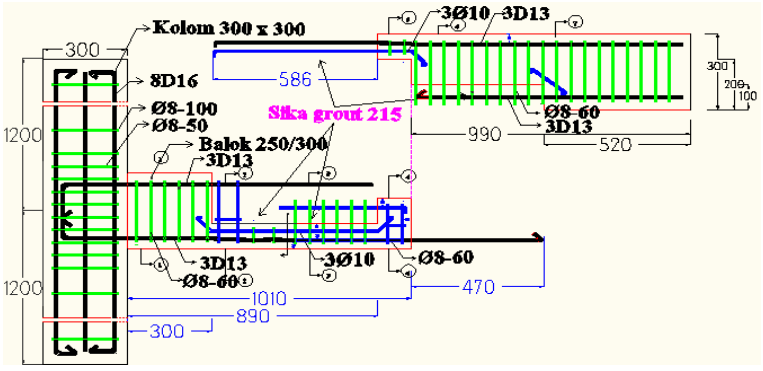

(c) STR-2

Fig. 3. Dimensions and details of test specimens.

3.3. Experimental Program

The experimental program consisted of three specimen beam-column joints. Each specimen is tested by cyclic loading in a predetermined load order. Hydraulic jack with a capacity of 50 tons and a screw jack with a capacity of 20 tons are used to apply lateral loading. cyclic lateral forces applied to the top of the upper column. The maximum drift ratio is 7.34%, and each drift is loaded three times. Linear Variable Differential Transformer (LVDT) and dial gauge are used to measure downward and upward movement of beams and columns. The cyclic load applied to the specimen refers to ACI recommendation 374.1-2005. drift ratio plan and test setup for cyclic loading at the beam-column connection can be seen in Fig. 4

Fig. 4. Test setup

4. RESULTS AND FINDINGS

4.1. Load - Deflection Behaviour.

Fig. 5 shows the relationship between lateral load and displacement. Table 3 shows the maximum load values for push and pull conditions. For monolith and str-1 specimens, the maximum load capacity is 19.6 kN and 13.4 kN. Displacement at the maximum load on both specimens is 147.95 mm. This indicates ductile behavior. When the displacement exceeded 147.95 mm, the lateral load decreased steadily due to yielding of the longitudinal reinforcement. For the specimen STR-2, the maximum load was 17.81 kN and displacement at maximum load was 189.37 mm. The load increased until the displacement reached 70.95 mm after that it decreases, and increase again at displacement 115.58 mm. After peak load, the strength decreases as the number and width of bending cracks and shear cracks increase. from the results of the strength and displacement test show that the maximum strength of the STR-1 and STR-2, less than monolit, at the same peak displacement. The hysteresis loop graph of all test specimens shows a fat hysteresis model, showing that the specimens did not undergo material disintegration during loading. Despite experiencing an intermediate lateral shear ratio, the specimen is still able to achieve the minimum required drift ratio of 3.5% without experiencing a significant decrease in lateral load capacity.

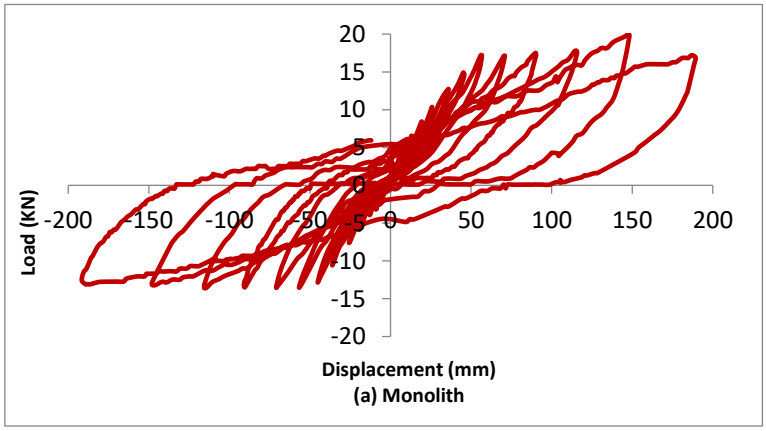

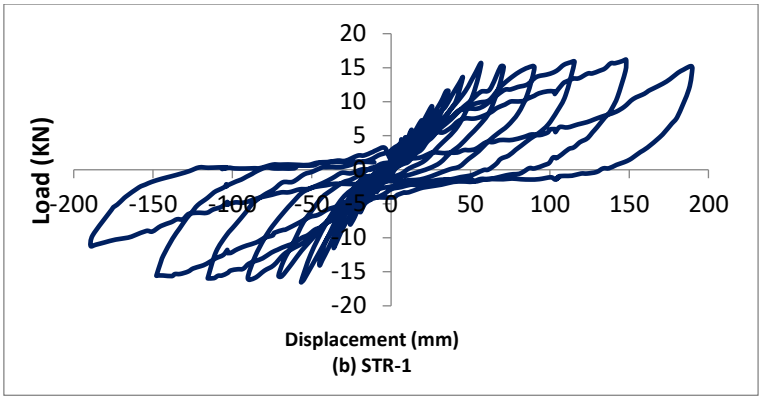

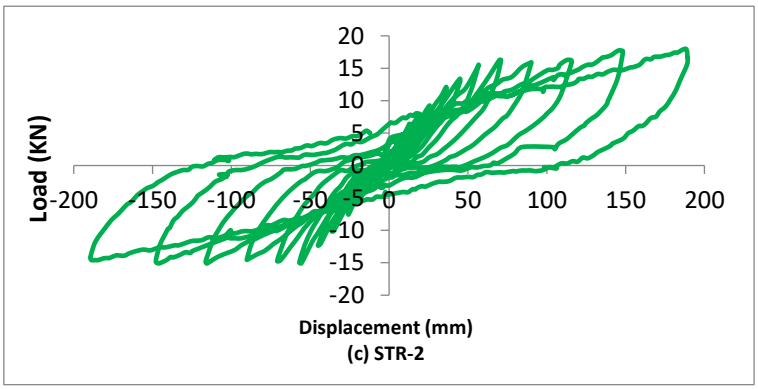

Fig. 5. Load displacement hysteretic curve

Table 3. Experimental Results

DRIFT	Disp. (mm)	Monolit		STR-1		STR-2	
		Maximum Load in kN		Maximum Load in kN		Maximum Load in kN	
		forward cycle (+)	reverse cycle (-)	forward cycle (+)	reverse cycle (-)	forward cycle (+)	reverse cycle (-)
0,20%	**5,16**	3,45	2,205	3,735	0,99	3,525	1,11
0,25%	**6,45**	4,2	2,52	4,47	2,16	4,05	1,89
0,35%	**9,03**	5,01	3,21	4,785	3,285	4,785	2,295
0,50%	**12,9**	6,54	3,945	5,82	4,425	6,36	3,345
0,75%	**19,35**	8,4	5,805	7,2	6,21	7,665	5,61
1,00%	**25,8**	10,32	7,59	9,345	7,995	9,18	7,575
1,40%	**36,12**	12,66	10,59	11,55	11,445	12,105	10,185
1,75%	**45,15**	14,91	12,795	13,53	14,04	13,365	12,345
2,20%	**56,76**	16,9	13,8	15,63	16,53	15,555	15,03
2,75%	**70,95**	17,115	13,5	15,105	15,57	16,245	14,67
3,50%	**90,3**	17,2	13,35	15,03	15,915	15,9	14,535
4,48%	**115,58**	17,7	13,35	15,84	15,96	16,23	15,105
5,73%	**147,95**	19,6	13,4	16,215	15,585	17,7	15,09
7,34%	**189,37**	17,2	13,09	15,21	11,175	17,805	14,325

4.2. Energy Dissipated Capacity

The energy dissipation graph and the input energy for each load cycle are presented in Fig. 6. A comparison of the dissipation energy values of the test specimens is presented in Fig. 7. Seen in each monolithic specimen, STR-1 and STR-2, the dissipation energy tends to increase due to an increase in drift level, but for each repetition cycle at each drift level, the same amount of dissipation energy tends to decrease. This is caused by the development

of cracks at the same drift level which is relatively constant (no significant new cracks have formed) or only the cracking widening occurs at the same location. The monolith energy dissipation graph has a sharp increase after passing the 3.5% drift ratio level while STR-1 and STR-2 have experienced a sharp increase after passing the 2.75% drift ratio level then the loop cycles that are formed become increasingly large so that the accumulation of energy that can be absorbed and scattered along the cyclic loading also increases. Based on Table 4 the energy dissipation of STR-1 up to a drift of 3.5%, is more stable compared to monolith and STR-2 specimens. This can be seen from the amount of cumulative dissipation energy due to the thrust and pull force at STR-1 is greater than the monolith and STR-2. The total energy of the cumulative dissipation of STR-1 at a drift of 3.5% was 2,102.44 KNmm, while the monolith and STR-2 specimens were 1,528.57 KNmm and 1,993.38 KNmm. At a 7.34% drift (end of test), significant decrease in dissipation energy occurs in STR-1 specimens, this occurs because the beam experiences a high degree of strength degradation due to the wide flexural shear cracking at the beam-column junction. Whereas STR-2 looks more stable. This can be seen from the cumulative dissipation energy value at STR-2 greater than monolith and STR-1.

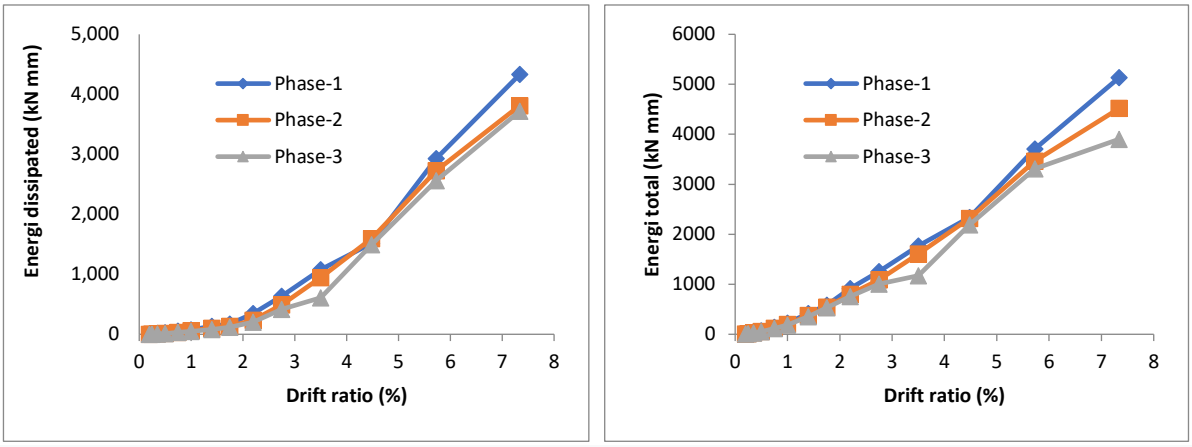

(a). Monolith

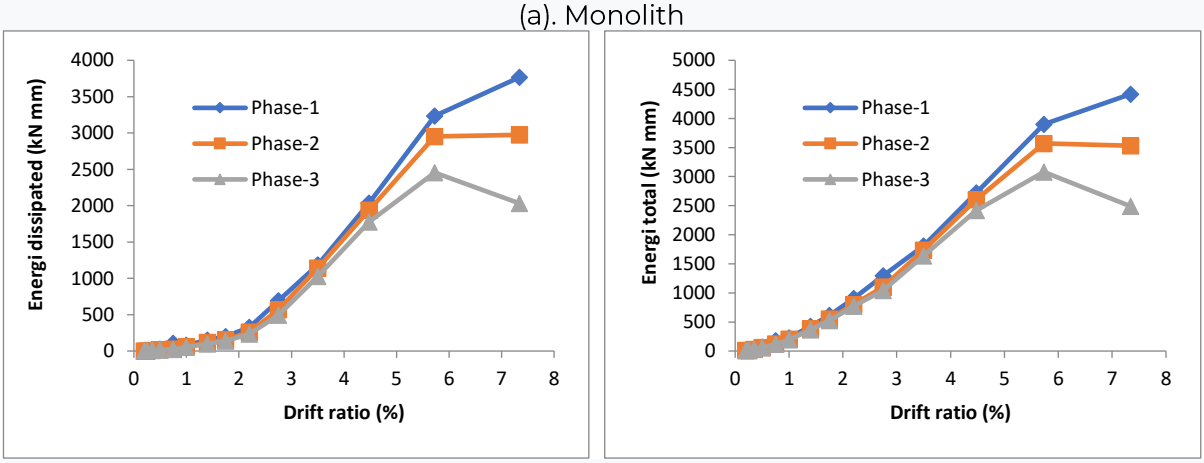

(b). STR-1

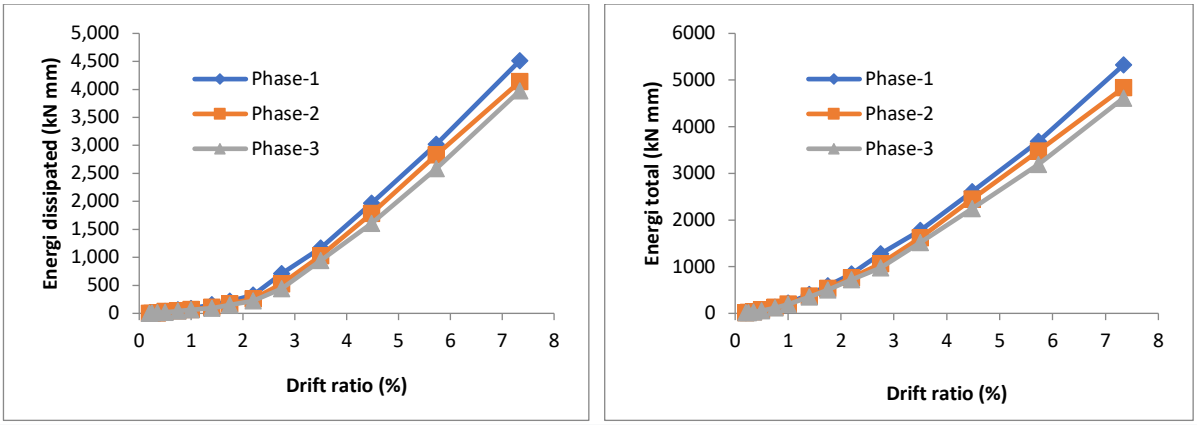

(c). STR-1

Fig. 6. Comparison of Input Energy and Dissipation Energy

Table 4. Energi Dissipation Result

DRIFT	MONOLITH		STR-1		STR-2	
	Total	Kumulatif	Total	Kumulatif	Total	Kumulatif
0,20%	0,90	0,90	2,16	2,16	2,41	2,41
0,25%	1,61	2,51	5,62	7,78	4,68	7,09
0,35%	5,22	7,73	10,21	17,99	10,02	17,11
0,50%	12,34	20,06	15,44	33,42	16,91	34,02
0,75%	31,23	51,29	24,74	58,16	40,33	74,35
1,00%	48,32	99,62	52,64	110,81	62,14	136,49
1,40%	81,04	180,66	96,43	207,23	92,76	229,25
1,75%	116,84	297,50	136,45	343,68	147,69	376,94
2,20%	204,18	501,68	236,05	579,73	226,11	603,05
2,75%	418,49	920,17	493,49	1.073,22	443,93	1.046,98
3,50%	608,40	1.528,57	1.029,23	2.102,44	946,40	1.993,38
4,48%	1.494,31	3.022,88	1.774,87	3.877,31	1.609,37	3.602,75
5,73%	2.562,93	5.585,81	2.454,59	6.331,90	2.585,42	6.188,16
7,34%	3.721,00	9.306,80	2.031,44	8.363,34	3.975,99	10.164,15
	9.306,80		8.363,34		10.164,15	

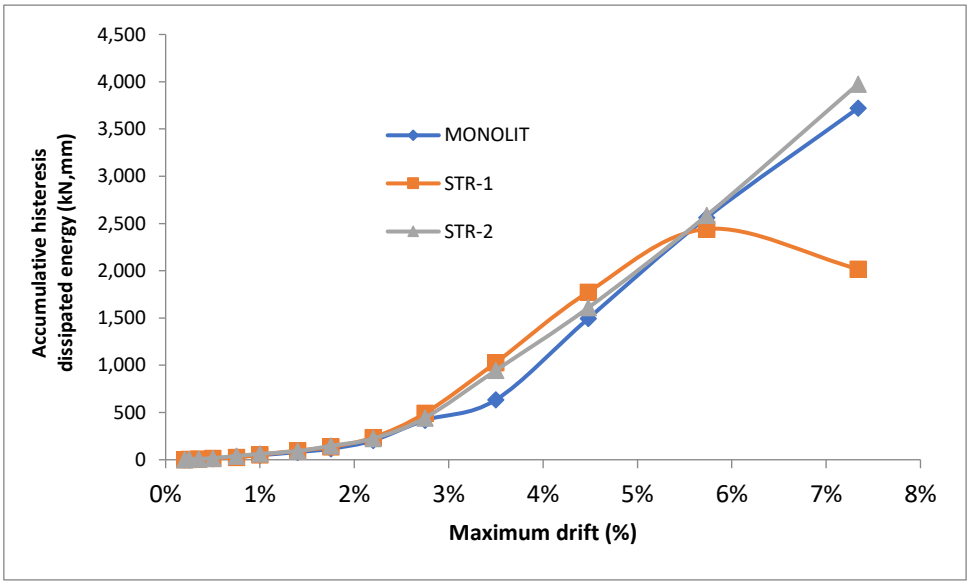

Fig. 7. Energy dissipation fungsi drift ratio

Table 5. Relative Energi Dissipation

Spesimen	Ideal Energy dissipation (kN-mm)		Actual Energy dissipation (kN-mm)		relative energy dissipation ratio (β)	
	drift 3.5%	drift 7.34%	drift 3.5%	drift 7.34%	drift 3.5%	drift 7.34%
Monolith	608,4	3.721	3112,6	9066,7	0,195	0,410
STR-1	1.029,23	2.031,44	3103,4	8251	0,332	0,246
STR-2	946,40	3.975,99	3228,5	9587,4	0,293	0,415

Referring to the results of tests that have been done, the relative dissipation energy ratio β in the three test objects, where β is defined according to equation 4 above, shows values greater than 1/8 (0.125), so they still meet the criteria required by ACI 374.1-05 or it mean the structure still has the ability to maintain its stability before it collapses.

5. CONCLUSION

1. Compared to monoliths, the STR-1 capacity to hold thrust loads is lower by 17.27%, while for tensile loads it increases 19.10%. If averaged, an STR-1 increase of 0.917% will be obtained. Whereas for STR-2 the thrust load that can be held decreases by 9.15% and increases by 12.73% for the tensile force compared, and when averaged it will be obtained an increase in STR-2 by 1, 78%. The same crack pattern occurs in all three specimens, namely flexural cracking of the beam at a low cycle, and then widening to a shear flexural crack at a higher cycle. while in the column, it starts with flexural cracks at low cycles, then sloping cracks appear which turn into shear cracks at higher cycles.
2. Cumulative energy dissipation achieved by STR-1 specimens at a minimum drift ratio of 3.5% as required by ACI 374.1-05, an increase of 69.17% compared to Monolith specimens. While the 7.34% drift ratio decreased -45.4%. The amount of cumulative energy dissipation that can be achieved STR-2 specimens at a drift ratio of 3.5%, increased by 55.60% and at a 7.34% drift ratio increased by 6.85%. compared to Monolith specimens. STR-2 specimens appear to be more able to maintain their strength against the effects of cyclic impulses and pull loads up to a 7.34% drift (end of test), compared to monoliths and STR-1.
3. Relative energy dissipation β in the three test specimens shows values greater than 1/8 (0.125), so they still meet the criteria required by ACI 374.1-05 or in other words the three specimens still have the ability to maintain their stability before collapsing.

Reference:

1. ACI Commite 374, 2005, Acceptance Criteria for Moment Frames Based on Structural Testing and Commentary (ACI 374.1-05), American Concrete Institut.
2. Jamal, Mardew, Parung, Herman, Wihardi, Tjaronge dan Sampebulu, Victor. 2014. Ductility of Precast Concrete on Interior Beam-Column Joints Under Cyclic Loading. Proceedings of the 2nd International Seminar on Infrastructure Development. Balikpapan 3 – 4 Juni.Indonesia.
3. SNI 03-2847-2002, 2002, Tata Cara Perhitungan Struktur Beton untuk Bangunan Gedung. Badan Standarisasi Nasional.

4. Bonneau, O., Poulin, C., Dugat, J., Richard, P., Aitcin, P.C., 1996, Reactive Powder Concretes, From Theory to Practice. Concrete International, 18 (4), 47-49.
5. SNI 03-1726-2002, 2002, Tata Cara Perencanaan Ketahanan Gempa untuk Bangunan Gedung, Badan Standarisasi Nasional.
6. Park, R and Paulay, T., 1975, Reinforced Concrete Structures, Canada: John Wiley.
7. Tjahyono, Elly dan Purnomo, Heru (2004). Pengaruh Penempatan Penyambungan pada Perilaku Rangkaian Balok-Kolom Beton Pracetak Bagian Sisi Luar. Makara, Teknologi. Vol.8, No.3.
8. Richard, P., 1996, Reactive Powder Concrete: A New Ultra High Strength Cementitious Material, 4th International Symposium on Utilization of High Strength/High Performance Concrete, 1343-1349.
9. Richard, P., Cheyrezy, M.H., 1994, Reactive Powder Concrete with High Ductility and 200–800 MPa Compressi Strength, Concrete Technology: Past, Present, Future, 144, 507-518.